

PAPER • OPEN ACCESS

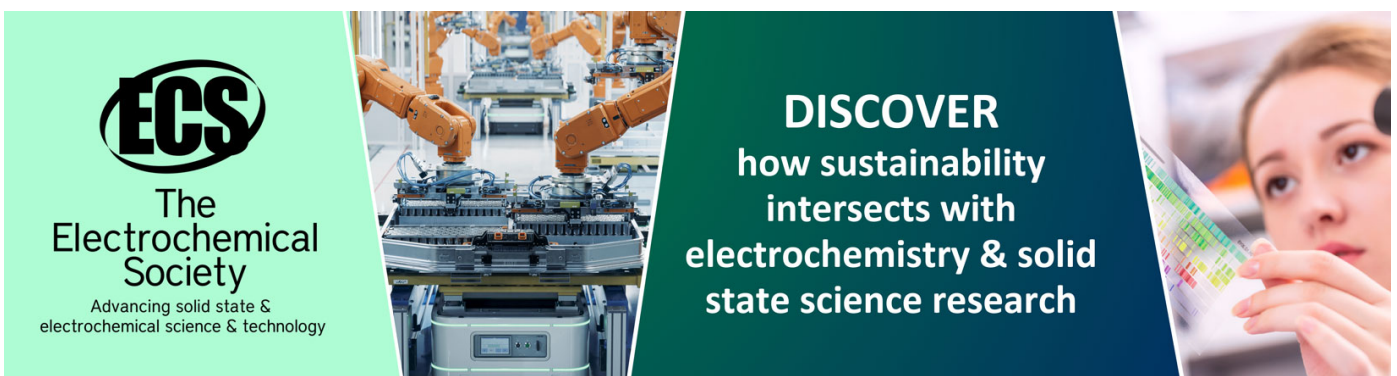
## Experimental and Numerical Analyses of Different Boundary Conditions on Composite Spherical Shell Cup by using APDL programmed

To cite this article: Fathi A. Al-Shamma and Ban Hussein Kassab 2020 *IOP Conf. Ser.: Mater. Sci. Eng.* **745** 012085

View the [article online](#) for updates and enhancements.

You may also like

- [Mesoscale strain and damage sensing in nanocomposite bonded energetic materials under low velocity impact with frictional heating via peridynamics](#)  
Krishna Kiran Talamadupula, Stefan J Povolny, Naveen Prakash et al.
- [Impact source identification in finite isotropic plates using a time-reversal method: experimental study](#)  
Chunlin Chen, Yulong Li and Fuh-Gwo Yuan
- [A gun recoil system employing a magnetorheological fluid damper](#)  
Z C Li and J Wang



**ECS**  
The  
Electrochemical  
Society  
Advancing solid state &  
electrochemical science & technology

**DISCOVER**  
how sustainability  
intersects with  
electrochemistry & solid  
state science research

# Experimental and Numerical Analyses of Different Boundaries Conditions on Composite Spherical Shell Cup by using APDL programmed

Fathi A. Al-Shamma<sup>1</sup>, Ban Hussein Kassab<sup>2</sup>

<sup>1</sup> Mechanical Engineer Dept. -College Eng. -Baghdad University, E-mail: fathyalshamma@gmail.com.

<sup>2</sup> Mechanical Engineer Dept. -College Eng. -Baghdad University, E-mail: eng.banhussien83@gmail.com

**Abstract.** Many researches have been done to obtain the factors that affect the value of the natural frequency for composite shell. The free vibration of composite spherical shell cap under impact loading is investigated in this study. The analysis is carried out theoretically using the higher-order shear deformation theory for composite spherical shell under impact loading, the results obtained was compared with numerical analysis using APDL program in the ANSYS software and experimentally using the hummer impact testing system and sigview program. The effects of radius of curvature, Thickness and boundary conditions (built in, quarter built in (arc), simply supported) on the basic frequency of orthotropic composite spherical shell cap have been investigated. The results show the dynamic characteristic it must be seen the rate of decreasing or increasing in the natural frequency of the composite material to take into consideration the effect of duration of impact loading on the dynamic properties of spherical composite shell. Selective composite material and its composition are 50% (0-90) woven fiber glass and 50% polyester resin.

## 1. Introduction

Fiber-reinforced plastic-coated composites are widely used in aerospace and other applications due to their high rigidity, high specific strength, and low specific density. Composites, in form of shell, find applications in the other industries. The Spherical shells are used in many structures such as pressure vessels, aerospace, vehicles, roof domes and submarines. so, free vibration of composite spherical shell cap is an important problem in order to get the natural frequency. Trupti Mahapatra [1] studied free vibration behavior for laminated composite spherical shell panel under the elevated hygrothermal environment. The matrix plate model was developed using Green - Lagrange's nonlinear kinetics within the framework of higher order shear deformation theory.

Tornabene [2] showed a comparison of classical 2D and 3D elements (FEs), classical and refined two-dimensional (GDQ) differential quadratic methods (GDQ) and a precise three-dimensional solution and thus the study of free vibration analysis of the one-layered and multi-layered layers about isotropic composite Sandwiches, spherical and cylindrical shell panels. SarmilaSahoo [3] analyzed free vibration problems of laminated composite stiffened shallow spherical shell panels with cutouts using



a finite element method. Fiorenza A [4] determined an exact free vibration analysis for doubly-curved laminated composite shallow shells have been carried out by combining the higher order shear deformation theory (HSDT) and a dynamic stiffness method (DSM). H. Nguyen-Van [5] reported that a numerical analysis of the free vibration of laminated composite shell/plate structures using the framework of the first-order shear deformation theory (FSDT). K.S. Sai Ram, T. Sreedhar Babu [6] investigated the free vibration of composite spherical shell cap without and with a cutout by using finite element method depending on the higher-order shear deformation theory. The free vibration of the laminated shell of the revolution was studied by Sheinman and Greif [7] using the Hamilton vibration principle. Results were presented mostly for cylindrical shells. Chandrasekhara [8] demonstrated the free vibratory properties of the double-curved composite shells using the finite element method. The formula is based on a first-class shear deformation theory that extends Sanders' shell theory of thinly curved shells. Narasimhan and Alwar [9] studied the free vibration of an articular annular spherical shell with boundary conditions fixed in both edges using the Chebyshev-Galerkin spectral method.

In this study the impact loading has been induced in the higher order shear deformation theory for composite spherical shell with different radius of curvature and used in simply supported, clamped and partially supported edges.

## 2. Theoretical Analysis

### 2.1 Higher order laminated shear deformation shell theory

The high-order laminated-shell theory included the displacement within the plane ( $u, v$ ) and extending up to the maximum cube in the term thickness ( $z$ ), and the transverse displacement ( $w$ ) which was considered as a constant through the plate thickness. This was done to take in to account parabolic variation for the transverse shear stresses through thickness of the plate Bose, P. and Reddy, J.N. [11].

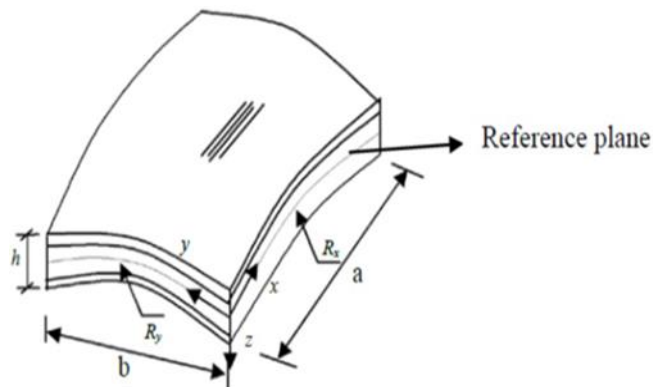


**Figure 1.** laminated composite doubly curved shell element

$$u(x, y, z, t) = u_0(x, y, t) + z \left[ Q_x(x, y, t) - \frac{4}{3} \left( \frac{z}{h} \right)^2 (Q_x(x, y, t) + \frac{\partial w}{\partial x}(x, y, t)) \right] \quad (1)$$

$$v(x, y, z, t) = v_0(x, y, t) + z \left[ Q_y(x, y, t) - \frac{4}{3} \left( \frac{z}{h} \right)^2 (Q_y(x, y, t) + \frac{\partial w}{\partial y}(x, y, t)) \right] \quad (2)$$

$$w(x, y, z, t) = w_0(x, y, t)$$

The constitutive relations for any layer in the  $(x, y)$  can be expressed in the form:

$$\begin{Bmatrix} \sigma_x \\ \sigma_y \\ \tau_{xy} \end{Bmatrix}_k = \begin{bmatrix} Q_{11} & Q_{12} & Q_{16} \\ Q_{21} & Q_{22} & Q_{26} \\ Q_{16} & Q_{26} & Q_{66} \end{bmatrix} \begin{Bmatrix} \epsilon_x^o \\ \epsilon_y^o \\ \gamma_{xy}^o \end{Bmatrix} + z \begin{Bmatrix} R_x \\ R_y \\ R_{xy} \end{Bmatrix} + z^3 \begin{Bmatrix} S_x \\ S_y \\ S_{xy} \end{Bmatrix} \quad (3)$$

$$\begin{Bmatrix} \tau_{yz} \\ \tau_{xz} \end{Bmatrix}_k = \begin{bmatrix} Q_{44} & Q_{45} \\ Q_{54} & Q_{55} \end{bmatrix}_k \begin{Bmatrix} Q_y + \frac{\partial w_o}{\partial y} \\ Q_x + \frac{\partial w_o}{\partial x} \end{Bmatrix} + 3z^2 \begin{Bmatrix} \theta_y \\ \theta_x \end{Bmatrix} \quad (4)$$

Where:  $\begin{Bmatrix} \theta_y \\ \theta_x \end{Bmatrix} = -\frac{4}{3h^2} \begin{Bmatrix} \frac{\partial w}{\partial y} + Q_y - A_1 \frac{v_o}{R_y} - A_1 \frac{u_o}{R_{xy}} \\ \frac{\partial w}{\partial x} + Q_x - A_1 \frac{u_o}{R_x} - A_1 \frac{v_o}{R_{xy}} \end{Bmatrix}$ ,  $\begin{Bmatrix} \epsilon_x^o \\ \epsilon_y^o \\ \gamma_{xy}^o \end{Bmatrix} = \begin{bmatrix} \frac{\partial u_o}{\partial x} + \frac{w_o}{R_x} \\ \frac{\partial v_o}{\partial y} + \frac{w_o}{R_y} \\ \frac{\partial u_o}{\partial y} + \frac{\partial v_o}{\partial x} + \frac{2w_o}{R_{xy}} \end{bmatrix}$

$$\begin{Bmatrix} R_x \\ R_y \\ R_{xy} \end{Bmatrix} = \begin{bmatrix} \frac{\partial Q_x}{\partial x} \\ \frac{\partial Q_x}{\partial y} \\ \frac{\partial Q_x}{\partial y} + \frac{\partial Q_y}{\partial x} \end{bmatrix}, \begin{Bmatrix} S_x \\ S_y \\ S_{xy} \end{Bmatrix} = \begin{bmatrix} \frac{\partial \theta_x}{\partial x} \\ \frac{\partial \theta_y}{\partial y} \\ \frac{\partial \theta_x}{\partial y} + \frac{\partial \theta_y}{\partial x} \end{bmatrix}$$

## 2.2 Virtual work

The equations of equilibrium are derived from higher order shell theory and again derived by using the principle of virtual displacement:

$$\partial W = \partial U + \partial V \quad (5)$$

Where:

$\partial U$  the virtual strain energy

$\partial V$  virtual potential energy.

Due to the transverse load  $q$  are given by:

$$\partial U = \int_{\Omega_0} \left[ \int_{-h/2}^{h/2} (\sigma_{xx} \partial \epsilon_{xx} + \sigma_{yy} \partial \epsilon_{yy} + \sigma_{xy} \partial \gamma_{xy} + \sigma_{xz} \partial \gamma_{xz} + \sigma_{yz} \partial \gamma_{yz}) dz \right] dx dy \quad (6)$$

$$\partial V = - \int_{\Omega_0} q \partial w_o dx dy \quad (7)$$

The value of  $\partial u$  could be written as:

$$\begin{aligned} \partial u = \int_{\Omega_0} (N_{xx} \partial \epsilon_x^o + M_{xx} \partial R_x - P_{xx} \partial S_x + N_{yy} \partial \epsilon_y^o + M_{xx} \partial R_y - P_{yy} \partial S_y + N_{xy} \partial \gamma_{xy}^o + \\ M_{xy} \partial R_{xy} - P_{xy} \partial \gamma_{xy} + Q_x \partial \gamma_{xx} - R_x \partial \gamma_{xz} + Q_y \partial \gamma_{yz} - R_y \partial \gamma_{yz}) dx dy \end{aligned} \quad (8)$$

And the value of  $N_{xx}, N_{yy}, N_{xy}, M_{xx}, M_{yy}, M_{xy}$  can be obtained from the following equations:

$$\frac{\partial N_{xx}}{\partial x} + \frac{\partial N_{xy}}{\partial y} = I_1 \frac{\partial^2 u}{\partial t^2} + \rho_2 \frac{\partial^2 Q_x}{\partial t^2} - \frac{4}{3h^2} I_4 \frac{\partial^2 (\frac{\partial w}{\partial x})}{\partial t^2} \quad (9)$$

$$\frac{\partial N_{xy}}{\partial x} + \frac{\partial N_y}{\partial y} = I_1 \frac{\partial^2 v}{\partial t^2} + \rho_2 \frac{\partial^2 Q_y}{\partial t^2} - \frac{4}{3h^2} I_4 \frac{\partial^2 (\frac{\partial w}{\partial y})}{\partial t^2} \quad (10)$$

$$\frac{\partial M_x}{\partial x} + \frac{\partial M_{xy}}{\partial y} - Q_x + \frac{4}{h^2} Q_x^* - \frac{4}{3h^2} \left( \frac{\partial M_x^*}{\partial x} + \frac{\partial M_{xy}^*}{\partial y} \right) = \rho_2 \frac{\partial^2 u}{\partial t^2} + \rho_3 \frac{\partial^2 Q_y}{\partial t^2} - \frac{4}{2h^2} \rho_5 \frac{\partial^2 (\frac{\partial w}{\partial x})}{\partial t^2} \quad (11)$$

$$\frac{\partial M_y}{\partial y} + \frac{\partial M_{xy}}{\partial x} - Q_y + \frac{4}{h^2} Q_y^* - \frac{4}{3h^2} \left( \frac{\partial M_y^*}{\partial y} + \frac{\partial M_{xy}^*}{\partial x} \right) = \rho_2 \frac{\partial^2 v}{\partial t^2} + \rho_3 \frac{\partial^2 Q_x}{\partial t^2} - \frac{4}{2h^2} \rho_5 \frac{\partial^2 (\frac{\partial w}{\partial y})}{\partial t^2} \quad (12)$$

$$\begin{aligned} \frac{\partial Q_x}{\partial x} + \frac{\partial Q_y}{\partial y} - \frac{4}{h^2} \left( \frac{\partial Q_x^*}{\partial x} + \frac{\partial Q_y^*}{\partial y} \right) + \frac{4}{3h^2} \left( \frac{\partial^2 M_x^*}{\partial x^2} + 2 \frac{\partial^2 M_{xy}^*}{\partial x \partial y} + \frac{\partial^2 M_y^*}{\partial y^2} \right) = I_1 \frac{\partial^2 w}{\partial t^2} - \frac{16}{9h^4} I_7 \left( \frac{\partial^2 w_{xx}}{\partial t^2} + \frac{\partial^2 w_{yy}}{\partial t^2} \right) + \\ \frac{4}{3h^2} I_4 \left[ \left( \frac{\partial^2 u_x}{\partial t^2} + \frac{\partial^2 v_y}{\partial t^2} + \frac{4}{3h^2} \rho_5 \left( \frac{\partial^2 (\frac{\partial Q_x}{\partial x})}{\partial t^2} + \frac{\partial^2 (\frac{\partial Q_y}{\partial y})}{\partial t^2} \right) \right) \right] - q(x, y, t) \end{aligned} \quad (13)$$

Where:

$$\rho_2 = I_2 \frac{4}{3h^2} I_4, \rho_5 = I_5 \frac{4}{3h^2} I_7, \rho_3 = I_3 \frac{4}{3h^2} I_5 + \frac{16}{9h^4} I_7$$

$$(I_1, I_2, I_3, I_4, I_5, I_7) = \sum_{k=1}^N \int_{z_k}^{z_{k+1}} \rho^{(k)} (1, z, z^2, z^3, z^4, z^6) \partial z$$

$$\begin{bmatrix} N_x & M_x & M_x^* \\ N_y & M_y & M_y^* \\ N_{xy} & M_{xy} & M_{xy}^* \end{bmatrix} = \sum_{L=1}^N \int_{h_L}^{h_{L+1}} \begin{bmatrix} \sigma_x \\ \sigma_y \\ \sigma_{xy} \end{bmatrix} (1, z, z^2) \partial z$$

$$\begin{bmatrix} Q_x & Q_x^* \\ Q_y & Q_y^* \end{bmatrix} = \sum_{L=1}^N \int_{h_L}^{h_{L+1}} \begin{bmatrix} \tau_{xz} \\ \tau_{yz} \end{bmatrix} (1, z^2) \partial z$$

For vibrating shells, one needs to include the kinetic energy of the shell. The kinetic Energy of a shell element of dimensions (dx, dy) and moving with velocity  $\frac{\partial w}{\partial t}$  is

$$\partial W = \frac{1}{2} \rho h \left( \frac{\partial w}{\partial t} \right)^2 \partial x \partial y \quad (14)$$

According to Hamilton's principle, then, the quantity to be minimized is now:

$$\partial u + \partial v - \partial W \quad (15)$$

Then the value of the natural frequency can be obtained depend on the boundary condition and the type of loading.

### 2.3 Theory of Impact Loading

Rate of change in speed during impact can be derived approximately from the expression as in [10].

$$m_1 \frac{dv_1}{dt} = -q \quad (16)$$

Where  $m_1$ ,  $v_1$  are the mass and the velocity of the impactor respectively

If the same distance indicates that the impactor and target are approaching the other due to local compression at the contact point, the velocity of this approach is:

$$\dot{\mu} = v_1 + v_2 \quad (17)$$

Where:

$\mu$  = the distance that the impactor and the target approach

$\dot{\mu}$  = the velocity of approach

$v_2$  = the change of velocity during impact

If the duration of impact is long then the hertzian law can be applied as:

$$q = n_1 \mu^{3/2} \quad (18)$$

Where:

$$n_1 = \frac{4\sqrt{R_1}}{3\pi(k_1 + k_2)}$$

Where:

$R_1$ : the radius of the impactor

$(k_1 + k_2)$  the constants depending on the properties of impactor and target.

Differentiating eq. (17) combining it with eq. (16) and substituting of eq (18) into the resultant equation yield:

$$\ddot{\mu} = -\frac{n_1}{m_1} \mu^{3/2} \quad (19)$$

$m_1$  is the mass of the impactor

If both sides of eq (19) are multiplied by  $(\dot{\mu})$  and the resultant equation is integrated then:

$$\dot{\mu}^2 - V^2 = -\frac{4}{5} \frac{n_1 \mu^{5/2}}{m_1} \quad (20)$$

Where:

$V$  the approach velocity of the two bodies at  $t=0$ .

$\mu_1$  the maximum deformation occurs

when ( $\mu' = 0$ ).

$$\mu_1 = \left[ \frac{5m_1 V^2}{4n_1} \right]^{2/5} \quad (21)$$

Substituting of eq. (21) into eq. (18) gives:

$$q = n_1^{2/5} \left[ \frac{5m_1 V^2}{4} \right]^{3/5} \quad (22)$$

This value of  $q$  will be substituted in the potential energy of eq (7) which depend on the initial velocity of the impact or, its mass, the properties of the shell and its radius of curvature. So that the natural frequency will be derived from the potential energy and its values give different shape factor for the natural frequency.

### 3. Experimental Analysis:

Glass fiber (woven) is used as a reinforcing stage in the form of woven fabric and polyester resin is used as a matrix phase for the composite materials of the specimen. The steps of the fabrication of the composite shell by using hand layup process are explained in details below.

The mold used in the experimental test is made from aluminum was manufactured by using milling machine and consists of two half spherical parts (male-female). The diameters of the half spherical male which used in the experimental test are 20 and 25cm and thickness of 3, 4, and 5mm.



**Figure 2.** Manufacturing the orthotropic spherical composite shell cap

In order to prepare the orthotropic shell, the surface of the mold was cleaned to be ready for use by acetone and coated by wax. The amount of resin is uniformly spread on the mold by brush, then the first layer of mats is laid. The resin is spread uniformly over the first layer by means of brush, before the second layer of mat is laid a steel roller is used to roll over the fabric, to enhance wetting and impregnation, then the second layer of mat is laid. This process is repeated until all fabric layers are placed then pressing it by the female cap. The casting process is done at room temperature for approximately (8) hours, then finally removed from the mold to obtain a well-equipped composite casing as shown in Figure 2.

### 3.1 Mechanical properties

The mechanical properties of test elements, E-glass orthopedic fibers and polyester matrix are shown in Table 1. The composite shell has a volume fraction of 50% for fiber and 1737.5 kg/m<sup>3</sup>, also the elasticity modulus is 22 Gpa and poisson ratio is 0.27.

**Table 1.** Mechanical Properties of Fiber E-Glass and the Polyester Resin

Material	Properties	Value
<b>E-Glass fiber</b>	Elasticity modulus (GPa)	74
	Shear modulus (GPa)	30
	Density (kg/m <sup>3</sup> )	2600
	Poisson ratio	0.25
<b>polyester risen</b>	Elasticity modulus (GPa)	4
	Shear modulus (GPa)	1.4
	Density (kg/m <sup>3</sup> )	1200
	Poisson ratio	0.4

### 3.2 Vibration Test

The vibration test was performed on a composite orthopedic casing with a diameter (20cm, 25cm, 30cm) and different thickness (3mm, 4mm and 5mm), with three boundary conditions (SFSF, built in and quarter built in (arc)). The natural frequency and response are found in order to detect damage and characterize the material. The Impact hammer (780985-01) is used to excite the shell with an impulse signal that causes the composite spherical shell to vibrate.

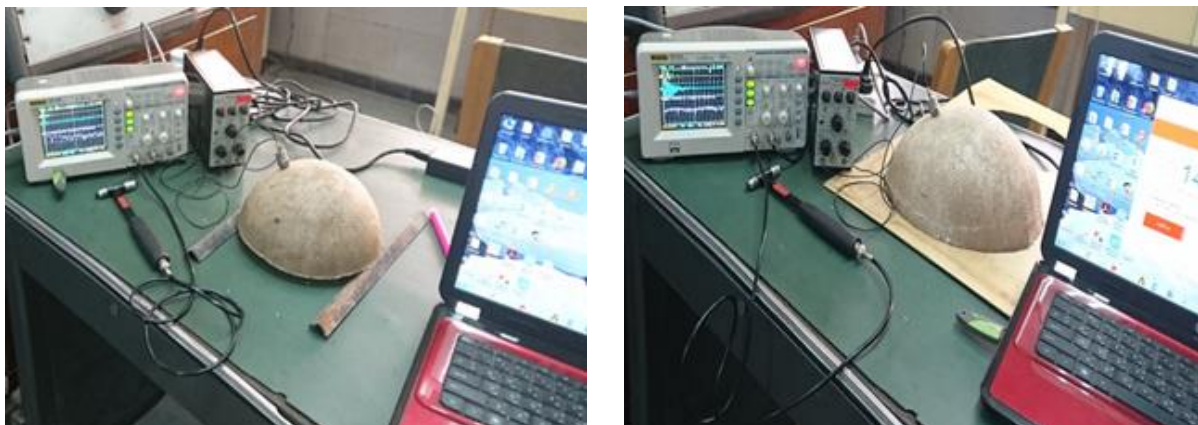


**Figure 3.** Vibration test rig of SFSF orthotropic composite shell cap with different supported

The Acceleration type (4368) is installed on the composite spherical casing, shell to capture the signal to the oscilloscope type (DS1102E). The oscilloscope is viewing the response of the sample that is loaded by the impact hammer which is connected to the oscilloscope and generates the excitation force on the composite spherical shell.

The oscilloscope device provided the signal as a peaked wave giving the natural frequency, as shown

in Figure 3. The results obtained from sigview program as shown in Figures 13, 14, and 15.

**4. Numerical solution**

This work using a FINITE ELEMENT PACKAGE is known as ANSYS package for numerical analysis is achieved in for orthotropic materials. A type of analysis is performed in the present work is the modal analysis which used to determine the natural frequencies and mode shapes of a structure. They are an important parameter in the design of a shell for a dynamic loading condition. The effects of the diameter, thickness and boundary conditions on the natural frequency had been studied numerically as in Figure 4, and 12. The importance of these figures showing the values of the fundamental's natural frequencies also the behavior of the first mode for different diameters and boundary conditions of shells.

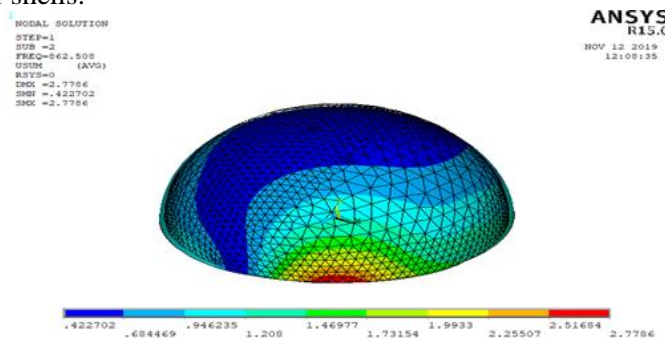


**Figure 4.** The Numerical Results for The First Mode of Orthotropic Composite Shell for Diameters (20cm, thickness 4mm, Simply Support)

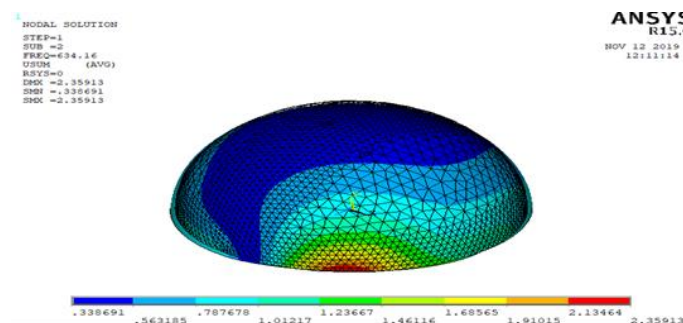


**Figure 5.** The Numerical Results for The First Mode of Orthotropic Composite Shell for Diameters (25cm, thickness 4mm, Simply Support)

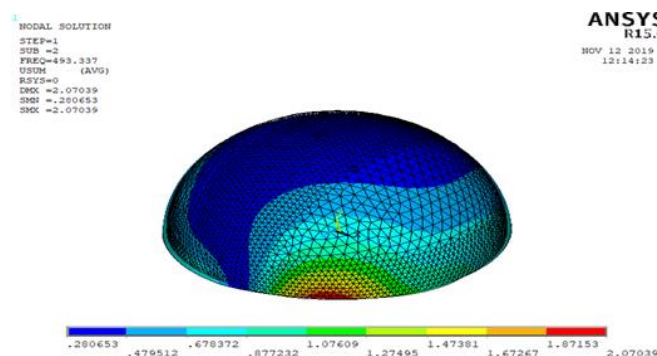


**Figure 6.** The Numerical Results for The First Mode of Orthotropic Composite Shell for Diameters (30cm, thickness 4mm, Simply Support)

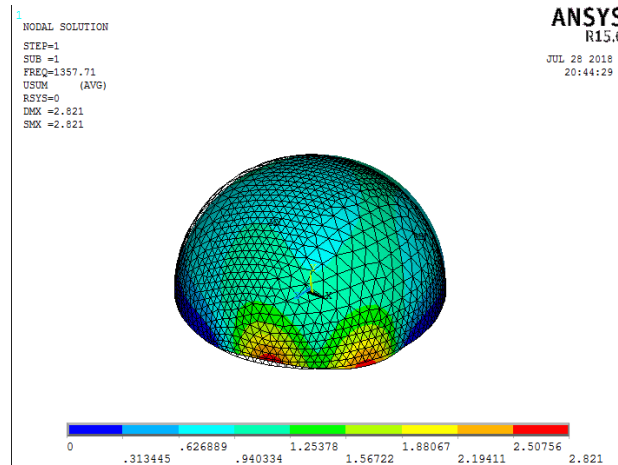


**Figure 7.** The Numerical Results for The First Mode of Orthotropic Composite Shell for Diameters (20cm, thickness 4mm, Arc Support)

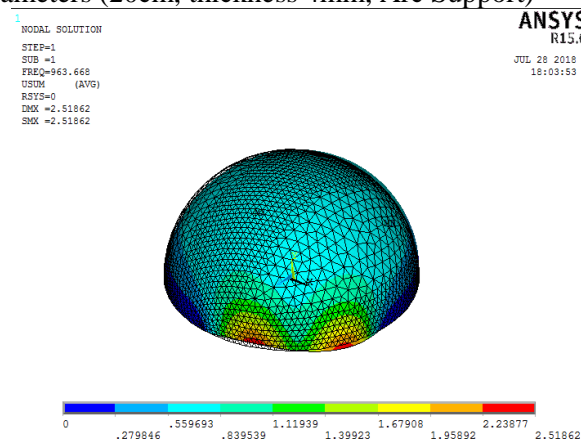


**Figure 8.** The Numerical Results for The First Mode of Orthotropic Composite Shell for Diameters (25cm, thickness 4mm, Arc Support)

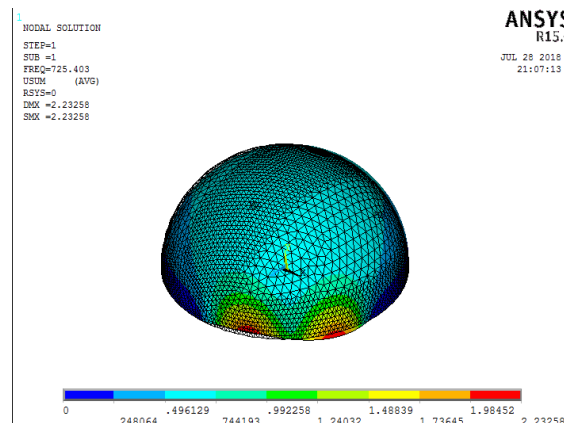


**Figure 9.** The Numerical Results for The First Mode of Orthotropic Composite Shell for Diameters (30cm, thickness 4mm, Arc Support)

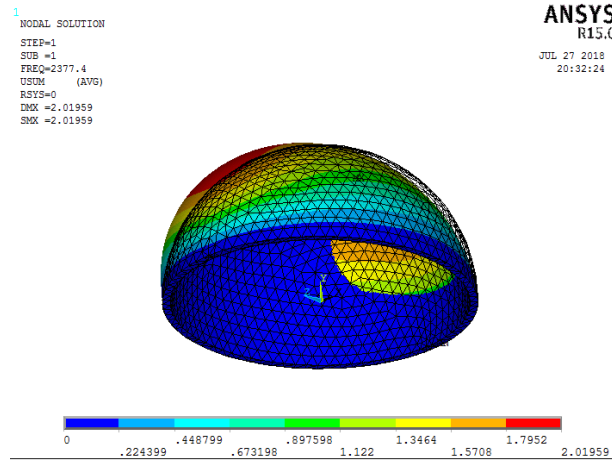


**Figure 10.** The Numerical Results for The First Mode of Orthotropic Composite Shell for Diameters (20cm, thickness 4mm, Built Support)

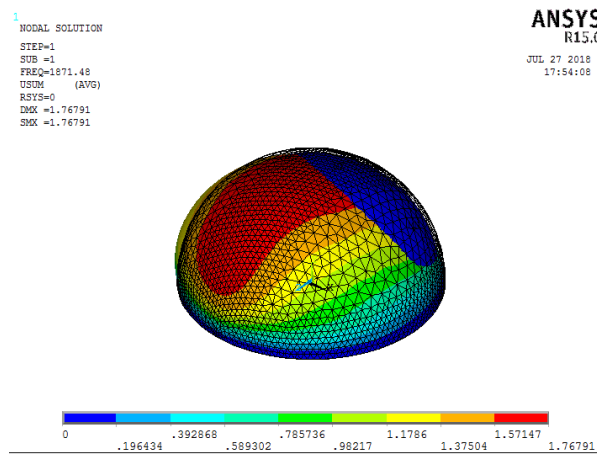


**Figure 11.** The Numerical Results for The First Mode of Orthotropic Composite Shell for Diameters (25cm, thickness 4mm, Built Support)

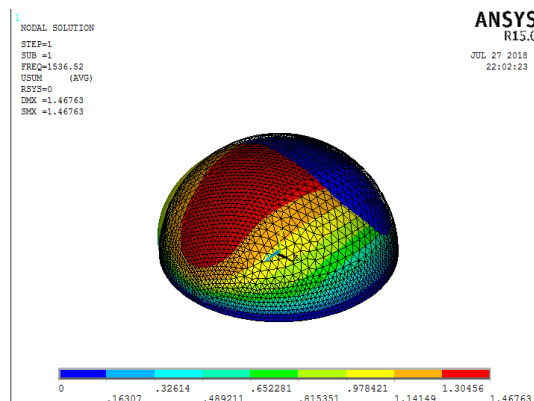


**Figure 12.** The Numerical Results for The First Mode of Orthotropic Composite Shell for Diameters (30cm, thickness 4mm, Built Support)

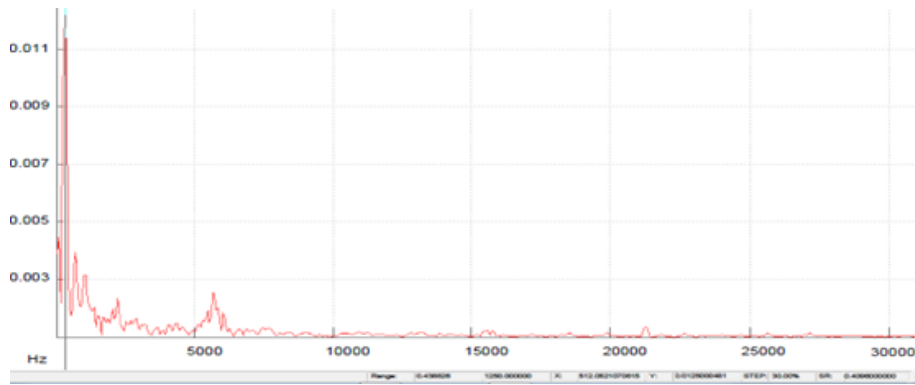


**Figure 13.** Experimental Response Spectrum of simply supported shell (diameter 25cm, thickness 4mm), [Sig view program]

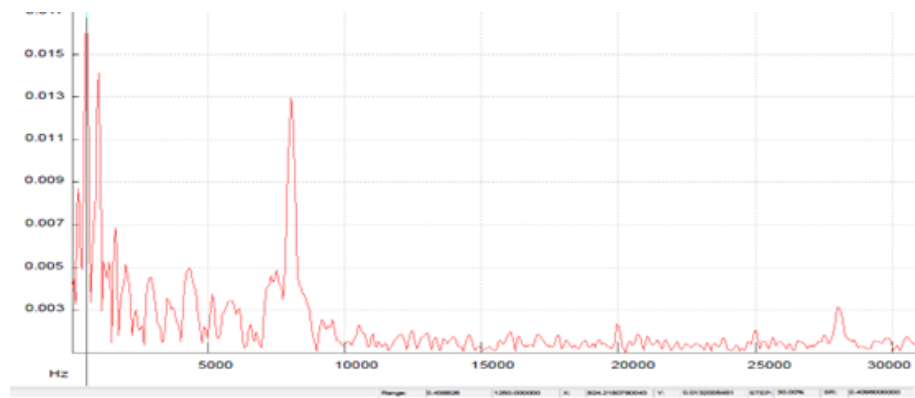


**Figure 14.** Experimental Response Spectrum of arc supported shell (diameter 25cm, thickness 4mm), [Sig view program]

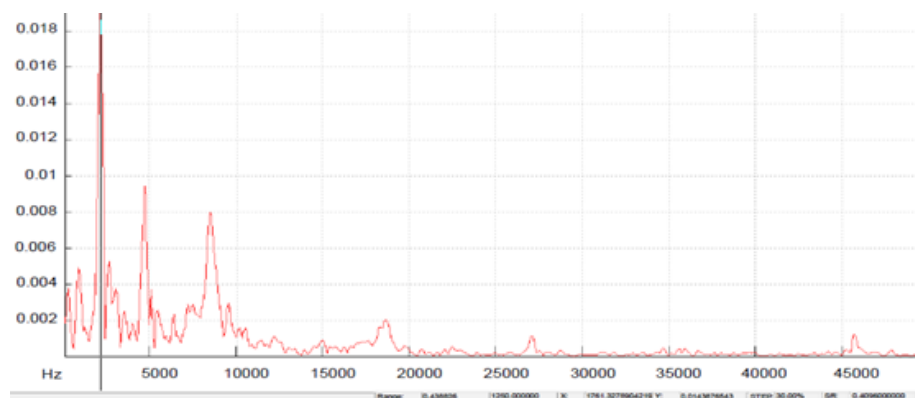


**Figure 15.** Experimental Response Spectrum of built supported shell (diameter 25cm, thickness 4mm), [Sig view program]

**Table 2.** Shows the theoretical, numerical and experimental results, also the percentage error between the theoretical and experimental results

	Diameter (cm)	Thickness (mm)	Frequency Theo. (HZ)	Frequency Num. (Hz)	Frequency Exp. (Hz)	Percentage error (%)
<b>Simply</b>	20	3	745.61	779.96	690.04	7.45
		4	762.32	862.51	743.02	2.53
		5	845.53	934.48	805.00	4.79
	25	3	499.82	567.54	453.04	9.35
		4	548.6	634.16	512.05	6.66
		5	600.32	690.06	565.03	5.87
	30	3	428.62	438.23	-	-
		4	441.32	493.34	-	-
		5	502.95	538.08	-	-
<b>Arc</b>	20	3	1149.8	1173.22	1073.25	6.65
		4	1298.6	1357.71	1224.43	5.71
		5	1430.98	1523.49	1340.26	6.33
	25	3	795.2	822.053	730.56	8.12
		4	889.73	963.668	824.21	7.36
		5	1047.13	1086.84	987.76	5.66
	30	3	600.54	622.842	-	-
		4	671.87	725.403	-	-
		5	755.81	773.428	-	-
<b>Built</b>	20	3	2260.33	2356.79	2237.67	1.00
		4	2280.81	2377.4	2250.53	1.32
		5	2301.97	2380.81	2265.14	1.59
	25	3	1775.64	1852.29	1750.32	1.42
		4	1790.53	1871.48	1761.32	1.63
		5	1818.28	1891.11	1780.111	2.09
	30	3	1500.01	1533.52	-	-
		4	1522.89	1536.52	-	-
		5	1548.97	1559.92	-	-

## 5. Results and Discussions

The main object of this study is to find the parameters that affect the value of the natural frequency for spherical composite shells, which are membrane with variable flatness ratio in the range of greater than 1/5 and thickness ratio between 1/10 to 1/50 which are thin shell, so in the dynamic characteristic it must be seen the rate of decreasing or increasing in the natural frequency of the composite material to take into consideration the effect of duration of impact loading on the dynamic properties of spherical composite shell. In the experimental analysis Figures 13,14 and 15 shows the effect of the boundary condition on the response spectrum for simply supported, arc supported and built in on the value of highest value of the maximum amplitude. It can be seen that the behavior of the response to the impact force is more stable for built in then the arc support and the simply support which is given more accurate result for the natural frequency. As shown in Figure 16 the results of the theoretical, numerical and experimental value of the natural frequency with the different thickness of composite material for diameter of 20 cm and simply supported for all edges is drawn between each two points as straight line to see the rate of increasing of the natural frequency. When transmitted from thickness 3 mm to 4 mm, the rate of increasing in the natural frequency is the same when transmitted from 4 mm

to 5 mm while there is difference in the negative rate in the numerical which have positive rate in the experimental results which coincide with the theoretical one that take the velocity of impact  $V$  in the calculation of the load. This effect has been studied in different diameter (25cm and 30 cm) as shown in Figures 17 and 18. The rate of increasing in the natural frequency is increased from thickness 4-5 mm more then 3-4 mm and increased with increasing diameters of shell for simply supported from all edges. This mean that the delaminating shear stress ( $\tau_{xz}, \tau_{yz}$ ) is more effect on the natural frequency when the diameter of the shell is increased. When the boundary condition will be replaced by ARC condition as shown in Figures 19, 20 and 21 it can be seen that there is an increasing in the rate of the behavior of the natural frequency and from negative to positive rate is also pronounced in transmission from thickness 4-5 mm with diameter 30 cm. This mean that there is a critical point which lower the natural frequency in the range of these thickness. In built in boundary condition shown in Figures 22, 23 and 24, because there is moment at the ends in addition to the supporting loads this will increased the effect of shear stress in the transverse direction causes increased in the value of natural frequency and clearly there is more effective of increasing in the rate of natural frequency in diameter of shell of 30 cm and when transmitted from 4-5 mm thickness. To illustrate the parameters that have more effect on the rate of increasing the natural frequency in spherical composite shell, Figures 25 to 33 give pronounced picture for increasing in diameter and especially in the built-in boundary condition. It can be seen the effect of the boundary condition for the same diameter on the point of changing the behaviour of frequency which is very important to give the change in the rate of natural frequency with orientation of the fibers in composite material.

In Figure 34 for 4mm thickness, the natural frequency for shell of diameter 20 cm in the three boundary conditions gives the maximum value, and the shell in the built-in support for the three diameter 20cm, 25cm, and 30cm has also the maximum value. The percentage error between theoretical and experimental results are given in table (3). In general, the value of the theoretical results is nearer to the experimental results then the numerical which depend on the modification in the representation of the impact loading and the max potential energy which varies with the duration of impact and the radius of the impactor and the target and the properties of the composite materials .

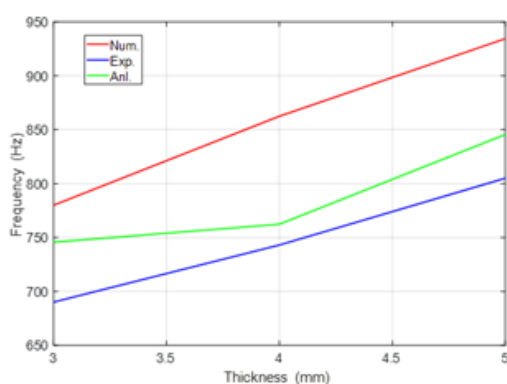


**Figure 16** Effect of thickness on the natural frequency (20cm-SFSF)

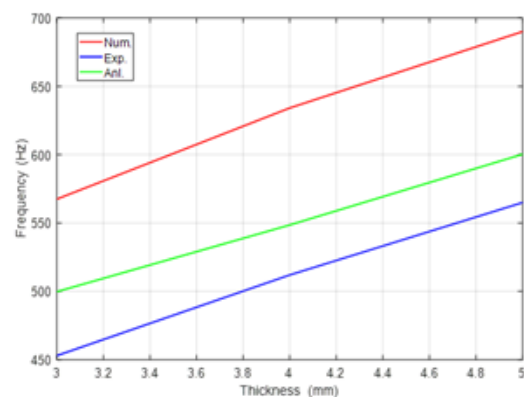


**Figure 17** Effect of thickness on the natural frequency (25cm-SFSF)

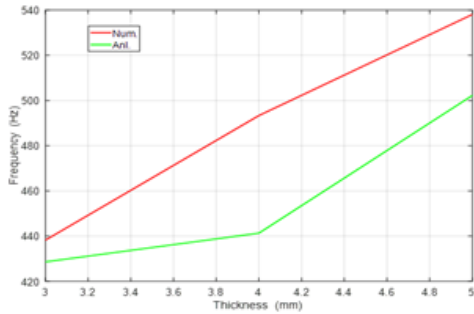


**Figure 18** Effect of thickness on the natural frequency (30cm-SFSF)

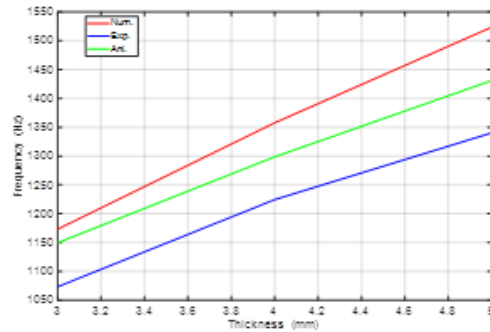


**Figure 19** Effect of thickness on the natural frequency (20cm-ARC)

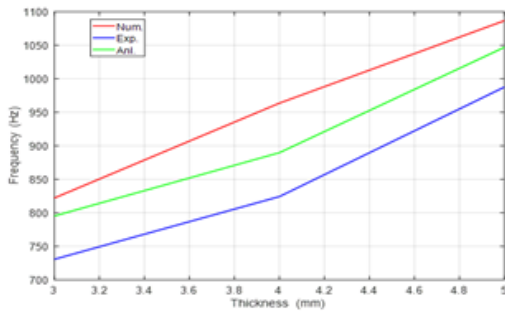


**Figure 20** Effect of thickness on the natural frequency (25cm-ARC)

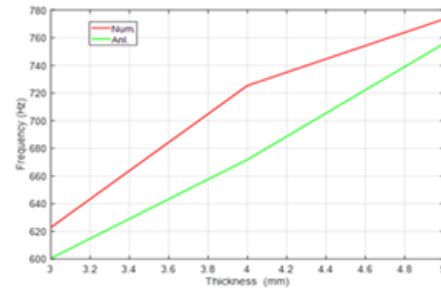


**Figure 21** Effect of thickness on the natural frequency (30cm-ARC)

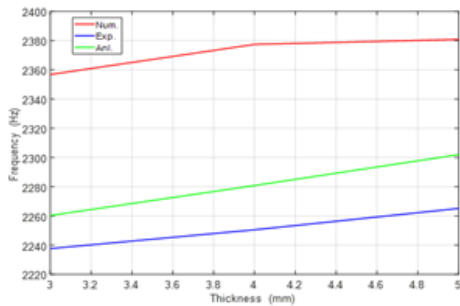


**Figure 22** Effect of thickness on the natural frequency (20cm-BULT)

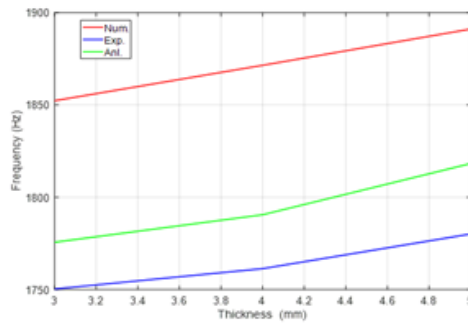


**Figure 23** Effect of thickness on the natural frequency (25cm-BULT)

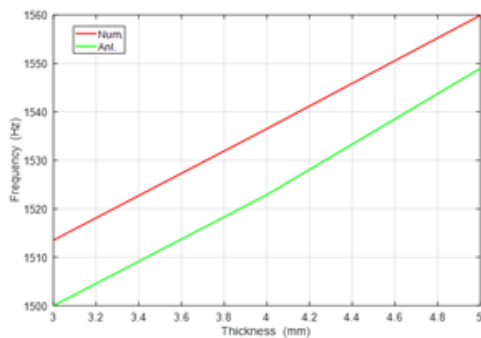


**Figure 24** Effect of thickness on the natural frequency (30cm-BULT)

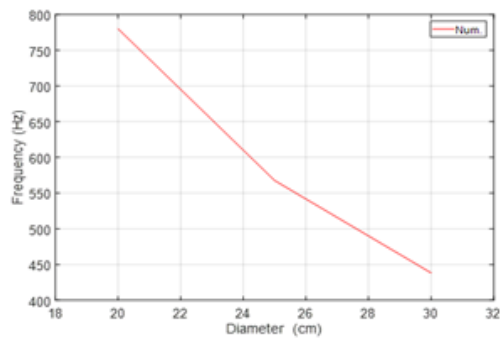


**Figure 25** Effect of DIM. on the natural frequency(THC.3mm-SFSF)

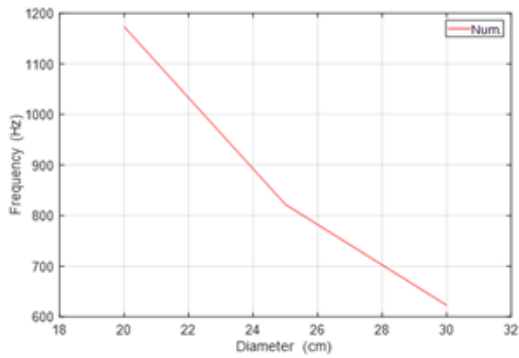


**Figure 26** Effect of DIM. on the natural frequency(THC.3mm-ARC)

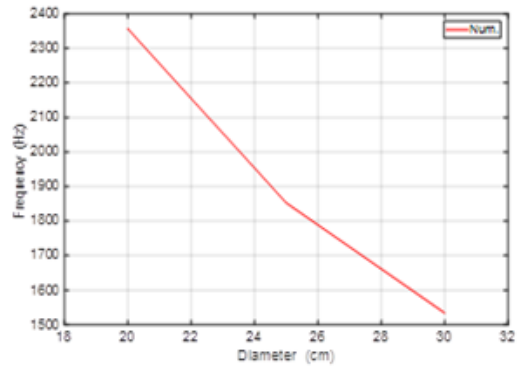


**Figure 27** Effect of DIM. on the natural frequency(THC.3mm-BULT)

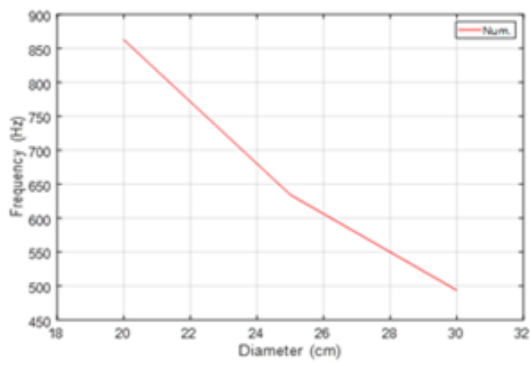


**Figure 28** Effect of DIM. on the natural frequency(THC.4mm-SFSF)

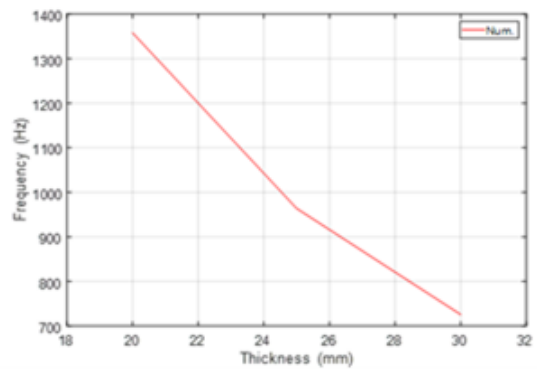


**Figure 29** Effect of DIM. on the natural frequency(THC.4mm-ARC)

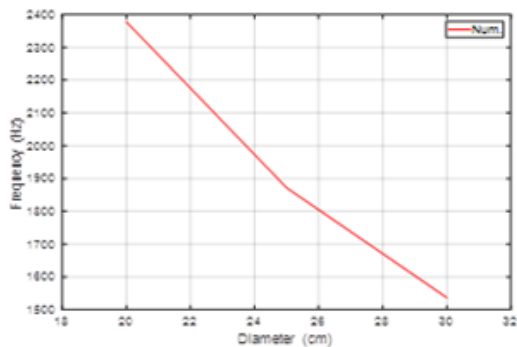


**Figure 30** Effect of DIM. on the natural frequency(THC.4mm-BULT)

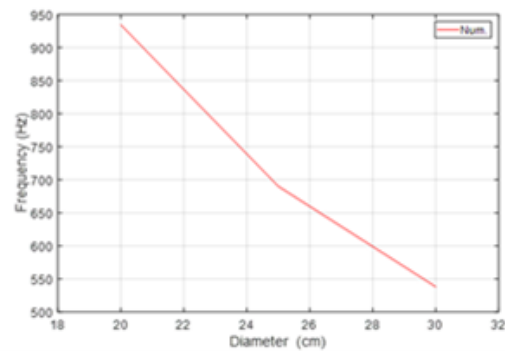


**Figure 31** Effect of DIM. on the natural frequency(THC.5mm-SFSF)

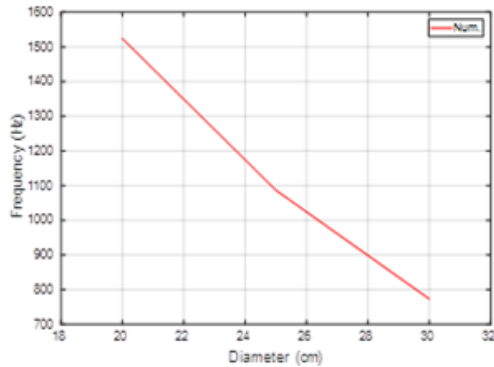


**Figure 32** Effect of DIM. on the natural frequency(THC.5mm-ARC)

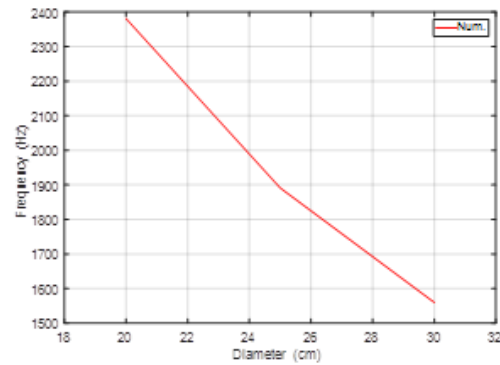


**Figure 33** Effect of DIM. on the natural frequency(THC.5mm-BULT)

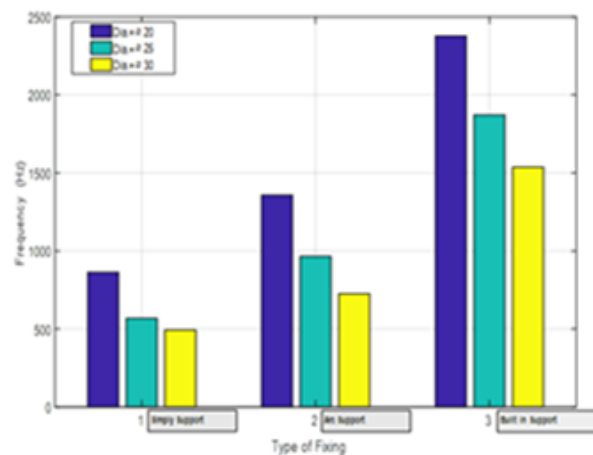


**Figure 34** the behavior of shell for 4mm thickness 20cm, 25cm, 30cm diameter (SFSF,ARC, BUILT) boundary conditions

## 6. Conclusions

Closed form solutions for obtain the factors that affect the value and the behavior of the natural frequency for composite shells with different boundary conditions. The results that obtained from using experimental spherical shell under impact loading and theoretical analysis using higher order shear deformation theory built for dynamic characteristic composite shell with numerical using APDL program in the ANSYS software for verification that:

- 1- The built-in condition gives more value in the natural frequency when compared with arc built in and simply supported but the behavior of the response is more stable
- 2- The rate of increasing in the response of simply supported is more pronounced than the other two conditions
- 3- There is a point that the behavior of the frequency will be changed which depend on the diameter of the shell for the same boundary conditions
- 4- There is a close agreement between the three methods used in the analysis of the results
- 5- in the numerical solution shell type 281 was used and in order to get the proper readings from

the program, the mesh distribution should be select (volume, free) depending on the element type for all boundary conditions (SFSF,ARC,BUILT)

## 7. Reference

- [1] Mahapatra, T.R. and Panda, S.K., 2016. Nonlinear free vibration analysis of laminated composite spherical shell panel under elevated hygrothermal environment: a micromechanical approach. *Aerospace Science and Technology*, *49*, pp.276-288.
- [2] Tornabene, F., Brischetto, S., Fantuzzi, N. and Viola, E., 2015. Numerical and exact models for free vibration analysis of cylindrical and spherical shell panels. *Composites Part B: Engineering*, *81*, pp.231-250.
- [3] Sahoo, S., 2014. Laminated composite stiffened shallow spherical panels with cutouts under free vibration—A finite element approach. *Engineering Science and Technology, An International Journal*, *17*(4), pp.247-259.
- [4] Fazzolari, F.A., 2014. A refined dynamic stiffness element for free vibration analysis of cross-ply laminated composite cylindrical and spherical shallow shells. *Composites Part B: Engineering*, *62*, pp.143-158.
- [5] Nguyen-Van, H., Mai-Duy, N. and Tran-Cong, T., 2008. Free vibration analysis of laminated plate/shell structures based on FSDT with a stabilized nodal-integrated quadrilateral element. *Journal of Sound and Vibration*, *313*(1-2), pp.205-223.
- [6] Ram, K.S. and Babu, T.S., 2002. Free vibration of composite spherical shell cap with and without a cutout. *Computers & structures*, *80*(23), pp.1749-1756.
- [7] Sheinman, I. and Greif, S., 1984. Dynamic analysis of laminated shells of revolution. *Journal of composite materials*, *18*(3), pp.200-215.
- [8] Chandrashekhara, K., 1989. Free vibrations of anisotropic laminated doubly curved shells. *Computers & structures*, *33*(2), pp.435-440.
- [9] Narasimhan, M.C. and Alwar, R.S., 1992. Free vibration analysis of laminated orthotropic spherical shells. *Journal of sound and vibration*, *154*(3), pp.515-529.
- [10] Zukas, J.A., Nicholas, T., Swift, H.F., Greszczuk, L.B., Curran, D.R. and Malvern, L.E., 1983. Impact dynamics. *Journal of Applied Mechanics*, *50*, p.702.
- [11] Reddy, J.N., 2003. *Mechanics of laminated composite plates and shells: theory and analysis*. CRC press.